RESEARCH ARTICLE

Mitochondria-mediated Apoptosis in Human Lung Cancer A549 Cells by 4-Methylsulfinyl-3-butenyl Isothiocyanate from Radish Seeds

Nan Wang[1], Wei Wang[2]*, Po Huo[1], Cai-Qin Liu[1], Jian-Chang Jin[1], Lian-Qing Shen[3]

Abstract

4-Methylsulfinyl-3-butenyl isothiocyanate (MTBITC) found in the radish (*Raphanus sativus* L.), is a well-known anticancer agent. In this study, the mechanisms of the MTBITC induction of cell apoptosis in human A549 lung cancer cells were investigated. Our PI staining results showed that MTBITC treatment significantly increased the apoptotic sub-G1 fraction in a dose-dependent manner. The mechanism of apoptosis induced by MTBITC was investigated by testing the change of mitochondrial membrane potential (ΔΨm), the expression of mRNAs of apoptosis-related genes by RT-PCR, and the activities of caspase-3 and -9 by caspase colorimetric assay. MTBITC treatment decreased mitochondrial membrane potential by down-regulating the rate of Bcl-2/Bax and Bcl-xL/Bax, and activation of caspase-3 and -9. Therefore, mitochondrial pathway and Bcl-2 gene family could be involved in the mechanisms of A549 cell apoptosis induced by MTBITC.

Keywords: 4-Methylsulfinyl-3-butenyl isothiocyanate - apoptosis - A549 cells - mitochondrial pathways

Asian Pac J Cancer Prev, **15 (5)**, 2133-2139

Introduction

The morbidity and mortality associated with lung cancer continues to increase, with 80% of all lung cancer patients suffering from non-small cell lung cancer (Chen, et al., 2008). Thus, an increased understanding of the molecular mechanisms useful for more effective and less harmful therapies is needed to reduce lung cancer mortality. Apoptosis is endogenous cell death program (Fisher, 1994). Tumors are characterized by uncontrolled proliferation and reduced apoptosis. Activation of apoptosis pathways is a key mechanism by which cytotoxic drugs kill cancer cells. Compounds which can induce apoptosis are considered to have potential as anti-tumoral agents (Frankfurt and Krishan, 2003).

Isothiocyanates (ITCs) are a family of compounds with potential cancer chemopreventive activities. Naturally-occurring ITCs found in Brassica vegetables, including benzyl ITC (BITC), phenethyl ITC (PEITC) and sulforaphane (SFN) have demonstrated anticarcinogenic activities. Consumption of Brassica vegetables containing ITCs is associated with decreased risk of cancer (Song et al., 2006; Razis and Noor, 2013; Karen-Ng et al., 2013). Radish is a member of the Cruciferae family of vegetables. 4-Methylsulfinyl-3-butenyl isothiocyanate (MTBITC), a compound from radish (Raphanus sativus L.), is a well-known anti-cancer agent active against liver and colon cancer cells. Our previous work has shown that MTBITC induced a dose-dependent decrease in viable A549 cells with an IC50 of 52.11±1.06 μM at 24 h (Fisher et al., 1995). Moreover, MTBITC has shown more specificity and sensitivity toward tumor cells compared with normal cells (Hanlon et al., 2007; Papi et al., 2008). MTBITC has been shown to induce detoxification enzymes in the human hepatocyte HepG2 cell line (Hanlon et al., 2007), and has interesting antioxidant/radical scavenging properties associated with a selective cytotoxic/apoptotic activity toward three human colon carcinoma cell lines (LoVo, HCT-116, and HT-29) (Papi et al., 2008). However, the mechanisms of how MTBITC induces apoptosis of human lung cancer cells are still not defined. Herein, we describe the investigation into the mechanisms responsible for the induction of apoptosis in A549 cells by MTBITC.

Materials and Methods

Chemicals

Radish (Raphanus sativus L.) seeds were obtained from Zhejiang Academy of agricultural sciences. All reagents and solvents used were of analytical and HPLC grade.

3-[4, 5-Dimethylthiazol-2yl]-2, 5-diphenyl tetrazolium

*[1]College of Biology and Environmental Engineering, Zhejiang Shuren University, [2]Institute of Quality and Standard for Agriculture Products, Zhejiang Academy of Agricultural Science, [3]College of Food Science and Biotechnology Engineering, Zhejiang Gongshang University, Hangzhou, China *For correspondence: wangwei5228345@126.com*

bromide (MTT), DMSO, Goldview and Rhodamine123 were purchased from Sigma (St. Louis, MO, USA). 2', 7'-Dichlorofluorescin diacetate (DCFH-DA) was from Molecular Probes (Eugene, OR, USA). Annexin V-FITC Apoptosis Detection Kits were from Oncogene (Boston, MA, USA), Caspase-3, and Caspase-9 colorimetric assay kits were from KeyGen (Nanjing KeyGen Biotech. Co. Ltd., Nanjing, China).

Isolation and purification of ITCs

MTBITC was extracted and purified from radish seeds according to the method described in literature with some modified with slight modifications (Ishii et al., 1989; Vaughn et al., 2005; Wang N et al., 2010). Briefly, ethyl acetate was used to extract the hydrolysis product from radish seed powder (1 Kg), and the non-polar part was removed with hexane. The ethyl acetate fraction (38 g) was subjected to silica gel chromatography, eluted by hexane/acetone (8:2, 7:3, 5:5, 4:6, 3:7, 2:8, v/v, 15 mL/min) to give four fraction. Fraction 2 was purified further by RP C-18 column chromatography to give compound 1 (203.7 mg). (analyzed by HPLC). The isolated compound (the purity was 98.5%) was identified as MTBITC by comparison of their spectral data (1H NMR, 13C NMR, and MS) with reported values (Kjaer et al., 1963; Kore et al., 1993; Bertelli et al., 1998; Vaughn and Berhow, 2005; Wang N et al., 2010).

MTBITC was prepared in sterilized dimethyl sulfoxide (DMSO) and stored at 4°C.

Cell culture

The human lung carcinoma cell line A549 (ATCC, Manassas, VA, United States) was cultured in RPMI-1640 medium (pH 7.0) supplemented with 10% fetal bovine serum (Gibco BRL, Grand Island, USA), 100 units/mL penicillin, and 100 μg/mL streptomycin sulfate. Cells were maintained at 37°C in an atmosphere of 5% CO_2.

Cell-cycle analysis

A549 cells (1×10^5 cells/mL) were seeded into a six-well plate, and then treated with MTBITC (0, 25, 50, 100 μM) for 24 h. After the treatment, adherent and floating cells were collected and washed by PBS, then fixed in ethanol (70% in PBS) maintained at 4°C for at least 12 h. The cells were washed with PBS, and then were stained with a propidium iodide (PI) fluorescent probe solution containing PBS, PI (50 μg/mL), and DNase-free RNase A (50 μg/mL) for 30 min in the dark. DNA fluorescence of PI-stained cells was evaluated by flow cytometry using an Epics Elite machine (Beckman Coulter Company, Fullerton, CA, United States). Cell distribution in the different phases of the cell cycle was analyzed by WinMDI 29.0 software.

Analysis of apoptosis cells

Cells were seeded into a six-well plate at a density of 1×10^5 cells/mL and were treated with MTBITC (0, 25, 50, 100 μM) for 24 h. After incubation, adherent and floating cell populations were combined, rinsed with PBS, and then resuspended in PBS containing 10% fetal bovine serum. The apoptosis rate of cells was determined by an Annexin V-FITC Apoptosis Detection Kit according to a modified manufacturer's protocol. Briefly, media binding reagent and Annexin V-FITC were added to the cells for 15 min in the dark. Cells were treated with binding buffer and PI, and then assayed by flow cytometry on an Epics Elite machine (Beckman Coulter Company) and analyzed by WinMDI 29.0 software.

Morphologic observations of apoptosis
Fluorescent microscopy observation

A549 cells were treated with MTBITC (0, 25, 50, 100 μM) for 24 h. They were fixed for 10 min in methanol:acetic acid (3:1) and washed with phosphate-buffered saline (PBS). They were stained with Hoechst 33258 stain solution (10 μg/mL) for 10 min, and washed with PBS. Stained cells were observed using a fluorescence microscope equipped with a 40× objective lens. Nuclear condensation and/or fragmentation were photographed.

Transmission electron microscopy (TEM)

A549 cells were treated with 50 μM of MTBITC for 24 h, and morphologic changes were assessed by transmission electron microscopy (TEM). Briefly, cells were harvested and fixed with 0.1 M 2.5% glutaraldehyde, and 2% paraformaldehyde in 0.1 M phosphate buffer (pH 7.4, 24 h), followed by 0.1% osmium tetroxide fixation (pH 7.2, 3 h at 4°C) and dehydration in an alcohol series (30%, 50%, 70%, 80%, 90% and 100%). Ultrathin sections were stained with uranyl acetate and lead citrate and observed under a JEM-1010 TEM (JEOL, Japan).

Detection of caspase catalytic activities

The activities of caspase-3 and -9 were assayed by the caspase colorimetric assay kits. The principle was based on the spectrophotometric detection of the chromophore p-nitroanilide (pNA) which was cleaved from the pNA-labeled peptide substrates, Ac-DEVD-pNA for caspase-3, and Ac-LEHD-pNA for caspase-9 (Pereira and Song, 2008; Xia et al., 2013). Briefly, after being treated with MTBITC (0, 12.5, 25, 50 μM) for 24 h, cells were harvested, washed with PBS, and resuspended in lysis buffer. Cell lysates were clarified by centrifugation at 10000 rpm for 1 min and kept on ice, then the protein concentration was determined using the BCA assay (Liu et al., 2005). A total of 50 μL cell lysate with 150 μg protein was incubated with 5 μL caspase substrate at 37°C for 4 h. The release of pNA was measured using a microplate reader (Tecan Group Ltd., Mannedorf, Switzerland) at 405 nm (Pereira and Song, 2008; Xia et al., 2013). Experiments were performed in triplicate.

Measurement of mitochondrial transmembrane potential ($\Delta\Psi m$) disruption

Rhodamine123 is a fluorescent dye that is incorporated into mitochondria in a $\Delta\Psi$m-dependent manner (Chen et al., 2007). A549 cells were cultured in a six-well plate at a density of 1×10^5 cells/mL and exposed to 50 μM MTBITC for 24 h. After treatment, the culture medium was replaced with a new medium containing 1 μM rhodamine123 for 30 min at 37°C in the dark. For fluorescence microscope observations, the cells were washed twice with PBS and

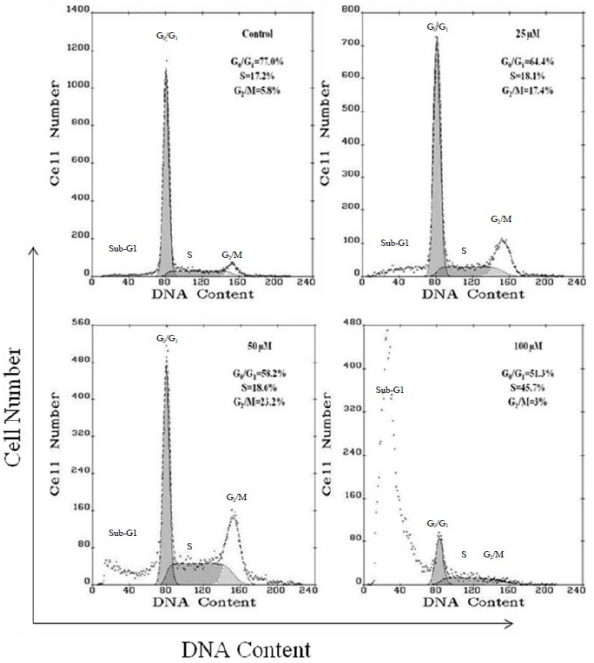

Figure 1. Inhibition of Cell Cycle Progress in A549 Cells were Treated with Various Concentrations of MTBITC for 24 h. Cells were fixed with ethanol and stained with PI, and then cell cycle distribution was analyzed by flow cytometry

the new culture medium was added. For quantitative analysis, cells were trypsinized, and quantified using flow cytometry and analyzed by WinMDI 29.0 software.

Isolation of total RNA and reverse transcription polymerase chain reaction (RT-PCR)

Expression of the apoptosis related genes, Bcl-2, Bcl-xL, and Bax, were studied by reverse transcriptase-PCR (RT-PCR). GAPDH was used as the control. Total RNA was isolated from untreated or treated A549 tumor cells with Trizol reagent (Invitrogen, USA). Reverse transcriptase reaction was performed from 1 μg of total RNA by M-MuLV reverse transcriptase (Toyobo, Japan) according to the manufacturer's recommendations. 2 μL RT product was used for the PCR reaction. The PCR reaction was carried out in a total volume of 20 μL containing 6 μL dH2O, 10 μL Master solution (Toyobo, Japan), 2 μL cDNA, and 1 μL primer. PCR was carried out using gene specific upstream and downstream primers. After initial denaturation at 94°C for 4 min, PCR amplification was performed as follows: 35 cycles of denaturation at 94°C for 30 s, annealing at 56°C for 30 s and strand extension at 72°C for 1 min. After a final extension at 72°C for 5 min, PCR products were resolved in 1% agarose gels and stained with Goldview.

Primer sequences were as follows: Bcl-2, 5'-TGTGGTATGAAGCCAGACC-3' (forward) and 5'-CAGGATAGCAGCACAGGATT-3' (reverse), Bcl-xL, 5'-CAATGGACTGGTGAGCCCA-3' (forward) and 5'-AGTTCAAACTCGTCGCCTG-3' (reverse), and Bax, 5'-CTGGGCCCCACAACTCAG-3' (forward) and 5'-TTCCCGCATCCACCGCACAC-3' (reverse) giving products of 154, 330, and 186 bp, respectively. Each reverse-transcribed mRNA product was internally controlled by

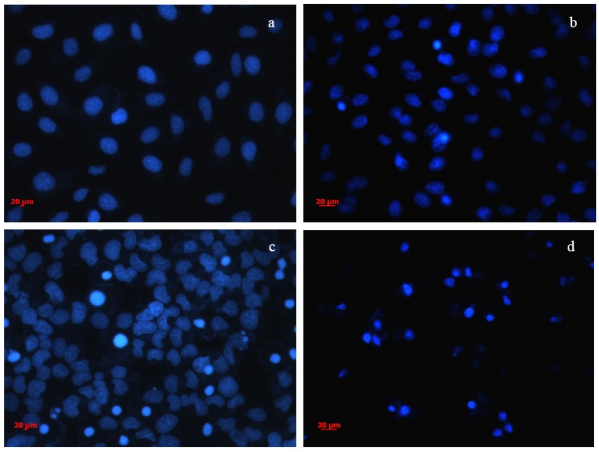

Figure 2. Morphological Changes in A549 Cells Treated with MTBITC for 24 h Followed by Hoechst 33258 Staining: (a) control; (b) 25 μM; (c) 50 μM; (d) 100 μM (Magnification, 40×)

glyceraldehyde-3-phosphate dehydrogenase (GADPH) PCR using primers 5'-CCCACTCCTCCACCTTTGAC-3' (forward) and 5'-TCTTCCTCTTGTGCTCTTGC-3' (reverse), yielding a 182 bp PCR product.

Statistical analysis

Data are means ± standard deviations (SD) of three replicate determinations. Analysis was by SPSS 16.0 (SPSS Incorporated, Chicago, IL, USA). One-way analysis of variance (ANOVA) and Duncan's new multiple-range test were used to determine differences among mean values. $P<0.01$ was considered significant.

Results

MTBITC increased sub-G1 populations and blocked the cell cycle in A549 cell

Investigation into the effects of MTBITC on cell cycle distribution was initiated to gain insight into the mechanisms of its anti-proliferative activity. A549 cells were treated with MTBITC and their distribution in the different phases of the cell cycle was calculated. At 24 h, cells treated with MTBITC (0, 25, 50, 100 μM) in the G2/M phase of the cell cycle increased from 5.8% to 23.2% in a dose-dependent manner (Figure 1). When treated with 100 μM of MTBITC, the S phase cells increased to 45.7%. The sub-G1 peak and the accumulation of cells in the G2/M and S phase were accompanied by a reduction in the G0/G1 phase in a dose-dependent manner after treatment with MTBITC for 24 h.

All these results indicated that MTBITC caused S phase or G2/M block. The block in cell cycle progression, therefore, likely contributed to MTBITC induced anti-proliferative effects. In addition, there was a significant increase in the sub-G1 fraction (hypodiploid DNA content), possibly due to cellular apoptosis.

MTBITC induces apoptosis on morphology in A549 cells

To further understand the anti-tumor effects of drug-loaded MTBITC, morphological changes of A549 cells treated with MTBITC were examined by

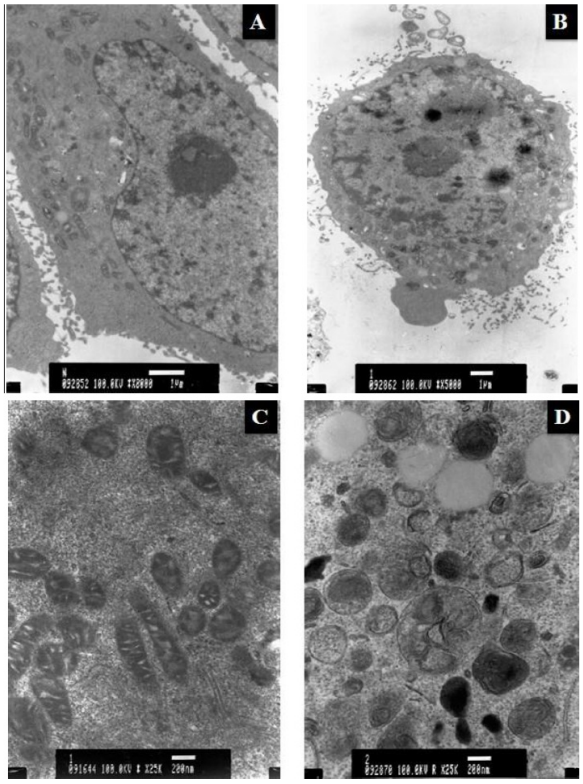

Figure 3. Apoptotic Features of A549 cell by TEM. (A and C) Untreated cells. (B and D) Cells were treated with 50 μM of MTBITC for 24 h, condensed chromatin, vacuoles, and swollen mitochondria were observed in cells. Magnification: (A) 2000×, (B) 5000×, (C and D) (Magnification, 25000×)

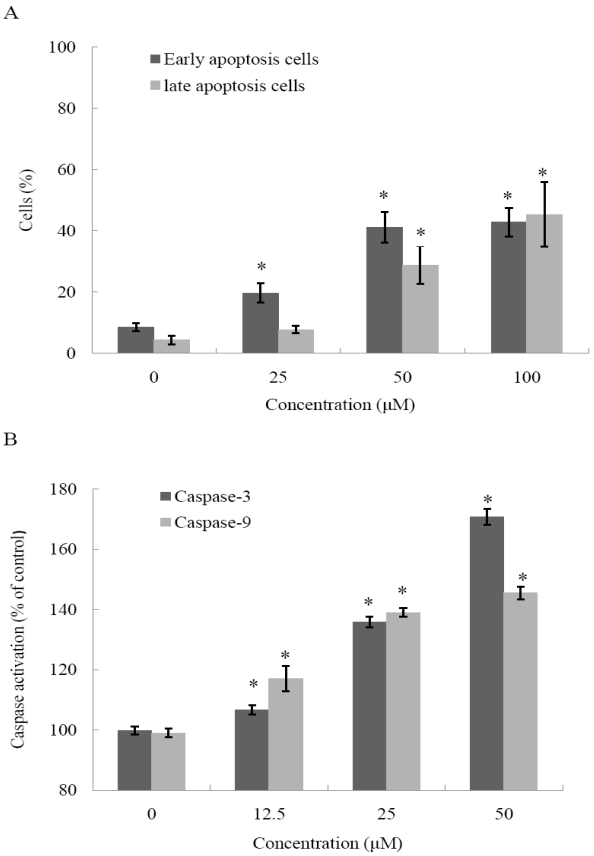

Figure 4. The Correlation of MTBITC-induced Apoptosis and Caspase Activation. (A) MTBITC induced apoptosis on A549 cells. Cells were incubated with MTBITC (0, 25, 50, and 100 μM) for 24 h. (B) MTBITC-induced caspase-3 and -9 activations in A549 cells. Cells were incubated with MTBITC (0, 12.5, 25, and 50 μM) for 24 h. Significant difference from control value was indicated by *($p < 0.01$)

fluorescence microscopy and TEM. Apoptotic cells were clearly observed (Figure 2), as they showed nuclear fragmentation, marked shrinkage, karyopyknosis, karyorrhexis, chromatin condensation and margination, stain darkening, cytomembrane folds, coiling and membrane blebbing, and apoptotic bodies.

The ultrastructures of A549 cells treated with MTBITC were shown in Figure 3. It is evident that control A549 cells were irregular in shape with randomly distributed organelles, the nuclei had finely granular and uniformly dispersed chromatin and a very big nucleolus, the mitochondria were intact, free ribosomes were observed, and many microvilli were seen on the cell surface (Figure 3A and 3C). When A549 cells were incubated with 50 μM MTBITC for 24 h, the ultrastructure of cells underwent significant changes compared to the control group. Treated cells began to show shrinkage, rounding, karyopyknosis, karyorrhexis, chromatin condensation, nuclear aberrations, apoptotic bodies, swollen mitochondria and vacuoles in the cytoplasm (Figure 3B and 3D).

MTBITC induced apoptosis in A549 cells by activation of caspases-3 and -9

The sub-G1 fraction appeared in the cell-cycle analysis, and the cells showed conventional morphological apoptotic signs when treated with MTBITC. In order to further confirm that MTBITC could induce cellular apoptosis, annexin V/PI double staining was done. Flow cytometry analysis of annexin V staining and PI accumulation was performed to differentiate early apoptotic cells (annexin V+ and PI-) from late apoptotic/necrotic cells (annexin V+ and PI+). A total of 27.4% of A549 cells were apoptotic when treated with 25 μM MTBITC for 24 h (19.68% were in early apoptosis plus 7.76% in late apoptosis/necrosis), 69.94% were apoptotic when treated with 50 μM (41.17% in early apoptosis plus 28.77% in late apoptosis/necrosis), and 88.11% were apoptotic when treated with 100 μM (42.77% in early apoptosis plus 45.34% in late apoptosis/necrosis). These results were significantly different to the control group (Figure 4A). Thus the results from the annexin V/PI double staining assay indicated that MTBITC could induce A549 cellular apoptosis.

It is well known that cellular apoptosis is generally associated with caspase activation. It has been established that caspases are the central executioners of the apoptotic pathway (Hengartner, 2000; Köhler et al., 2002; Sharifia et al., 2009). To evaluate whether the induced apoptotic effects of MTBITC were associated with caspase enzyme activation, we examined the activities of caspase-9 and caspase-3. MTBITC induced activation of caspase-3 and -9 in a dose-dependent manner, and a significant activation effect could be detected after incubation with 12.5 μM for 24 h. The activities of caspase-3 and caspase-9 were significantly increased in treated cells compared to controls (Figure 4B). These results indicated

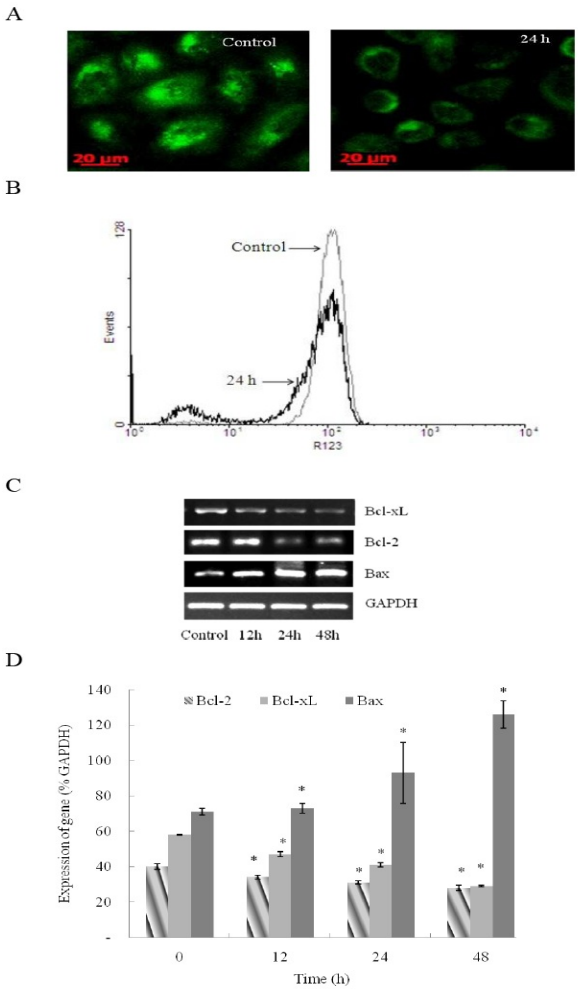

Figure 5. MTBITC Induced A549 Cells Apoptosis by Mitochondrial Pathway. (A) Cells were treated with 50 μM MTBITC for 24 h, and then stained with Rhodamine123, observed by Fluorescent Microscopy (Magnification, 40×). (B) Rhodamine123 stained A549 cells was obtained by Flow Cytometry. Grey line: non-treatment control, black line: 50 μM MTBITC treated cells for 24 h. (C) mRNA expression of Bcl-2, Bcl-xL, and Bax in A549 cells following exposure with 50 μM MTBITC for 0 h, 12 h, 24 h, 48 h. (D) Effect of MTBITC on mRNA level by RT-PCR assay. Data are shown by means ± SD (n = 3). *$P < 0.01$ vs. control

that MTBITC induced apoptosis was related to caspase activation. Caspase-9 plays a role as a major initiator of mitochondrial pathways, in turn, activating caspase-3 (Sharifia et al., 2009). Caspase 3 has been identified as a key mediator of apoptosis of mammalian cells (Kothakota et al., 1997). Thus, these results suggest that MTBITC induces mitochondrial changes in A549 cells.

MTBITC induced apoptosis via the mitochondrial pathway in A549 cells

To further investigate MTBITC induced apoptosis by a mitochondrial pathway in A549 cells, the effect of MTBITC on mitochondrial membrane potential (ΔΨm) was evaluated by rhodamine123 fluorescent staining. As expected, fluorescent microscopic observation revealed that a low amount of rhodamine123 was retained on A549 cells treated with 50 μM MTBITC for 24 h (Figure 5A). Moreover, quantitative measurement by flow cytometry showed that the fluorescent intensity in A549 cells was significantly decreased by MTBITC treatment (Figure 5B), suggesting that ΔΨm decreased.

During apoptosis, several pro-apoptotic and anti-apoptotic genes are involved in regulating the control of mitochondria (Li et al., 2008; Xi et al., 2012). Bcl-2, Bcl-xL, and Bax were detected by RT-PCR. As shown in Figure 5C and 5D, MTBITC treatment of A549 cells resulted in down-regulation of the expression of Bcl-2 and Bcl-xL, and up-regulation of the expression of Bax in a time-dependent manner. MTBITC did not affect the level of GAPDH when it was employed as a loading and internal control. These results suggest that MTBITC induces apoptosis in A549 cells via alteration of the Bax/Bcl-2 and Bax/Bcl-xL ratio.

Discussion

Epidemiological studies have shown that increasing dietary consumption of cruciferous vegetables may reduce cancer risk in humans (Li et al., 2008). The anti-carcinogenic effect of cruciferous vegetables is attributed to the presence of organic ITCs (Razis and Noor, 2013). Dietary ITCs found in cruciferous vegetables has been reported to reduce cancer risk by inducing phase II conjugating enzymes. (Karen-Ng et al., 2013; Zhu et al., 2013; Razis and Noor, 2013) MTBITC is a major phytochemical constituent of radish as well as other cruciferous vegetables with known chemopreventive properties. MTBITC has been shown to modulate the activity of phase II detoxification enzymes (Hanlon et al., 2007), suppress proliferation, and induce apoptosis in cancer cells (Papi et al., 2008), via pathways that have been suggested to be involved in anticarcinogenic processes. However, few studies have been carried out to ascertain the effects of MTBITC treatment in lung adenocarcinoma.

In our previous work, MTBITC displayed a strong antiproliferative activity toward A549 cells (Fisher et al., 1995). In the work reported herein, MTBITC induced both a dose- and time-dependent inhibitory effect on the proliferation of A549 cells. The IC50 value was 52.11 ± 1.06 μM at 24 h, 34.53 ± 0.37 μM at 48 h, and 15.43 ± 0.82 μM at 72 h. The IC50 values decreased with increasing incubation time (Wang et al., 2010). These studies suggested that MTBITC is a potent growth suppressing agent in A549 cells. Similar observations of different cytotoxic activities on various cancer cells have been made for sulforaphane, phenylethyl isothiocyanate (PEITC), and benzyl isothiocyanate (BITC) (Chiao et al., 2002; Conaway et al 2002; Hecht, 2000; Troncoso et al., 2005; Devi et al., 2012; Zhu et al., 2013). Normal lymphocytes can undergo cell death induced by drugs as a side-effect of chemotherapy aimed at malignant cells. Alessio Papi reported that Sulforaphane (SFN) caused a complete growth inhibition at 50 μM, whereas MTBITC showed only 15 (±5)% inhibition. It showed MTBITC with limited toxicity to normal human T-lymphocytes (Papi et al., 2008).

Using PI staining and flow cytometry analysis, our results indicated that MTBITC inhibited A549 cell proliferation by inducing S phase or G2/M growth arrest

(Figure 1). The appearance of the sub-G1 fraction and conventional morphological signs of apoptosis provided support for the idea that MTBITC induced apoptosis in A549 cells (Figure 1, Figure 2 and Figure 3). MTBITC-induced apoptosis was further confirmed by annexin V/PI double staining. The percentage of apoptotic cells increased in a dose-dependent manner (Figure 4A). These results indicated that the decrease in A549 cell viability by MTBITC was due to the modulation of the cell cycle and induction of apoptosis.

It is well established that apoptosis can occur by either the death-receptor pathway or the mitochondrial pathway. Both pathways are executed by caspases that are activated specifically in apoptotic cells (Ashkenazi and Dixit, 1998; Green and Reed, 1998; Okada and Mak, 2004; Philchenkov, 2004; Sharifia et al., 2009; Hsu et al., 2010 Milojkovic et al., 2013). J Renuka Devi reported that SFN down-regulated the expression of bcl-2 (antiapoptotic), while up-regulating p53 and Bax (proapoptotic) proteins, as well as caspase-3 (Devi et al., 2012). In this study, MTBITC treatment resulted in caspase-3 and -9 activation in A549 cells (Figure 4B), and in addition, observations indicated that the structure of the mitochondria was changed (Figure 3C and 3D), suggesting that a mitochondria-mediated mechanism plays an important role in apoptosis induction.

The pathway of apoptosis involves the participation of mitochondria, regulated by the antiapoptotic members of Bcl-2, and Bcl-xL, and proapoptotic members of Bax (Korsmeyer, 1999; Rahmani et al., 2013). Bcl-2 and Bcl-xL are found on the outer membranes of mitochondria and function in maintaining their integrity (Dewson and Kluck, 2010). Bax is found in a soluble form in the cytosol under normal conditions. In the presence of an apoptotic stimulus, Bax translocates from the cytosol to the mitochondria, which leads to the formation of membrane pores at the mitochondrial membranes, and thus, induces a decrease in the membrane potential ($\Delta\Psi m$) of the mitochondria (Kluck et al., 1997; Narita, et al., 1998; Eskes, et al., 1998; Antonsson et al., 2001; Basanez, et al., 2002). Bax promotes apoptosis by negatively regulating the antiapoptotic members of Bcl-2 and Bcl-xL and forming Bax/Bcl-2 or Bax/Bcl-xL heterodimers. The Bax/Bcl-2 or Bax/Bcl-xL ratio is a measure of the cell death switch, which determines whether a cell will live or die upon being exposed to an apoptotic stimulus (Sambaziotis et al., 2003; Dias and Bailly, 2005).

In the present study, a lower membrane potential was measured in cells from the treatment groups (Figure 5A, 5B) The expression of Bcl-2 and Bcl-xL were decreased, and the expression of Bax was increased (Figure 5C, 5D). Therefore, we concluded that MTBITC decreases the mitochondrial $\Delta\Psi m$ by increasing the ratio of Bax/Bcl-2 and Bax/Bcl-xL. The Bcl-2 family plays a key role in MTBITC induced apoptosis in A549 cells. These results indicate that MTBITC-induced apoptosis is associated with activation of caspases via the mitochondrial pathways in A549 cells.

In conclusions, MTBITC can inhibit the growth and induce the apoptosis of A549 cells. The mechanism is mediated by the activation of the mitochondrial death pathway, which requires the caspase cascade (via caspase-9 activating caspase-3), up-regulation of the ratio of Bax/Bcl-2 and Bax/Bcl-xL, and decreased the mitochondrial trans-membrane potential ($\Delta\Psi m$).

Acknowledgements

This research work was supported by the Zhejiang Provincial Natural Science Foundation of China (LQ13C200005) and National Natural Science Foundation of China (31101390).

References

Abdull Razis AF, Noor NM (2013). Cruciferous vegetables: dietary phytochemicals for cancer prevention. *Asian Pacific J Cancer Prev*, **14**, 1565-70.

Abdull Razis AF, Noor NM (2013). Sulforaphane is superior to glucoraphanin in modulating carcinogen-metabolising enzymes in Hep G2 Cells. *Asian Pac J Cancer Prev*, **14**, 4235-8.

Antonsson B, Montessuit S, Sanchez B, et al (2001). Bax is present as a high molecular weight oligomer/complex in the mitochondrial membrane of apoptotic cells. *J Biol Chem*, **276**, 11615-23.

Ashkenazi A, Dixit VM (1998). Death receptors: signaling and modulation. *Science*, **281**, 1305-8.

Basanez G, Sharpe JC, Galanis J, et al (2002). Bax-type apoptotic proteins porate pure lipid bilayers through a mechanism sensitive to intrinsic monolayer curvature. *J Biol Chem*, **277**, 49360-5.

Brinker AM, Gayland FS (1993). Herbicidal activity of sulforaphene from stock (Matthiola incana). *J Chem Ecol*, **19**, 2279-84.

Chen CY, Hsu YL, Tsai YC, et al (2008). Kotomolide A arrests cell cycle progression and induces apoptosis through the induction of ATM/p53 and the initiation of mitochondrial system in human non-small cell lung cancer A549 cells. *Food Chem Toxicol*, **46**, 2476-84.

Chen CY, Liu TZ, Liu YW, et al (2007). 6-Shogaol (alkanone from Ginger) induces apoptotic cell death of human hepatoma p53 mutant Mahlavu subline via an oxidative stress-mediated caspase-dependent mechanism. *J Agri Food Chem*, **55**, 948-54.

Chiao JW. Chung FL, Kancherla R, et al (2002). Sulforaphane and its metabolite mediate growth arrest and apoptosis in human prostate cancer cells. *Int J Oncol*, **20**, 631-6.

Conaway CC, Yang YM, Chung FL (2002). Isothiocyanates as cancer chemopreventive agents: their biological activities and metabolism in rodents and humans. *Curr Drug Metab*, **3**, 233-255.

Devi JR, Thangam EB (2012). Mechanisms of anticancer activity of sulforaphane from *Brassica oleracea* in HEP-2 human epithelial carcinoma cell line. *Asian Pacific J Cancer Prev*, **13**, 2095-2100.

Dewson G, Kluck RM (2010). Bcl-2 family-regulated apoptosis in health and disease. Cell Health and Cytoskeleton, 2, 9-22.

Dias N, Bailly C (2005). Drugs targeting mitochondrial functions to control tumor cell growth. *Biochem Pharmacol*, **70** (1):1-12.

Eskes R, Antonsson B, Osen-Sand A, et al (1998). Bax-induced cytochrome c release from mitochondria is independent of the permeability transition pore but highly dependent on Mg2+ ions. *J Cell Biol*, **143**, 217-24.

Fisher DE (1994). Apoptosis in cancer therapy: crossing the threshold. *Cell*, **78**, 539-42.

Fisher M, Golden NH, Katzman DK, et al. (1995). Eating disorders in adolescents: a background paper. *J Adolesc Health*, **16**, 420-37.

Frankfurt OS, Krishan A (2003). Apoptosis-based drug screening and detection of selective toxicity to cancer cells. *Anticancer Drugs*, **14**, 555-61.

Green DR, Reed JC (1998). Mitochondria and apoptosis. *Science*, **281**, 1309-12.

Hanlon PR, Webber DM, Barnes DM (2007). Aqueous extract from Spanish black radish (*Raphanus sativus* L. Var. niger) induces detoxification enzymes in the HepG2 human hepatoma cell line. *J Agric Food Chem*, **55**, 6439-46.

Hengartner MO (2000). The biochemistry of apoptosis. *Nature*, **407**, 770–6.

Hecht SS (2000). Inhibition of carcinogenesis by isothiocyanates. *Drug Metab Rev*, **32**, 395-411.

Hsu W, Lee B, Pan T (2010). Redmold dioscorea-induced G2/M arrest and apoptosis in human oral cancer cells. *J Sci Food Agric*, **90**, 2709-15.

Ishii G, Saijo R, Mizutani J (1989). A quantitative of 4-methylthio-3-butenyl glucosinolate in Daikon (*Raphanus sativus* L.) roots by gas liquid chromatography. *J Japan Soc Hort Sci*, **58**, 339-44.

Karen-Ng LP, Marhazlinda J, Abdul Rahman ZA, et al (2011). Effects of isothiocyanate intake, glutathione s-transferase polymorphisms and risk habits for age of oral squamous cell carcinoma development, *Asian Pacific J Cancer Prev*, **12**, 1161-6.

Kluck RM, Bossy-Wetzel E, Green DR, et al (1997). The release of cytochrome c from mitochondria: a primary site for Bcl-2 regulation of apoptosis. *Science*, **275**, 1132-6.

Kore AM, Spencer GF, Wallig MA (1993). Purification of the ω- (Methylsulfiny1)alkyl Glucosinolate Hydrolysis Products: 1-Isothiocyanato-3-(methylsulfinyl) propane, 1-Isothiocyanato-4-(methylsulfinyl) butane, 4-(Methylsulfinyl) butanenitrile, and 5- (Methylsulfinyl) pentanenitrile from Broccoli and *Lesquerella fendleri*. *J Agric Food Chem*, **41**, 89-95.

Korsmeyer SJ (1999). Bcl-2 gene family and the regulation of programmed cell death. *Cancer Res*, **59**, 1693s-1700s.

Kothakota S, Azuma T, Reinhard C, et al (1997). Caspase-3-generated fragment of gelsolin: effector of morphological change in apoptosis. *Science*, **278**, 294-8.

Köhler C, Orrenius S, Zhivotovsky B (2002). Evaluation of caspase activity in apoptotic cells. *J Immunol Methods*, **265**, 97-110.

Kjaer A, Ohashi M, Wilson JM, et al (1963). Mass spectra of isothiocyanates. *Acta Chemica Scandinavica*, **17**, 2143-54.

Li C, Wu H, Huang Y, et al (2008). 6-O-Angeloylenolin induces apoptosis through a mitochondrial/caspase and NF-kB pathway in human leukemia HL60 cells. Biomed Pharmacother, **62**, 401-9.

Liu MJ, Yue PY, Wang Z, et al (2005). Methyl protodioscin induces G2/M arrest and apoptosis in K562 cells with the hyperpolarization of mitochondria. *Cancer Lett*, **224**, 229-41.

Milojkovic A, Hemmati PG, Müer A, et al (2013). p14ARF induces apoptosis via an entirely caspase-3-dependent mitochondrial amplification loop. *Int J Cancer*, **133**, 2551-62.

Narita M, Shimizu S, Ito T, et al (1998). Bax interacts with the permeability transition pore to induce permeability transition and cytochrome c release in isolated mitochondria. *Proc Nati Acad Sci USA*, **95**, 14681-6.

Okada H, Mak TW (2004). Pathways of apoptotic and non-apoptotic death in tumour cells. *Nat Rev Cancer*, **4**, 592–603.

Papi A, Orlandi M, Bartolini G, et al (2008). Cytotoxic and Antioxidant Activity of 4-Methylthio-3-butenyl isothiocyanate from *Raphanus sativus* L. (Kaiware Daikon) Sprouts. *J Agric Food Chem*, **56**, 875-83.

Pereira NA, Song Z (2008). Some commonly used caspase substrates and inhibitors lack the specificity required to monitor individual caspase activity. *Biochem Biophys Res Commun*, **377**, 873-7.

Philchenkov A (2004). Caspases: potential targets for regulating cell death. *J Cell Mol Med*, **8**, 432-44.

Rahmani M, Aust MM, Attkisson E, et al (2013). Dual inhibition of Bcl-2 and Bcl-xL strikingly enhances PI3K inhibition-induced apoptosis in human myeloid leukemia cells through a GSK3- and Bim-dependent mechanisms. *Cancer Res*, **73**, 1340.

Sambaziotis D, Kapranos N, Kontogeorgos G (2003). Correlation of bcl-2 and bax with apoptosis in human pituitary adenomas. *Pituitary*, **6**, 127-33.

Song L, Iori R, Thornalley PJ (2006). Purification of major glucosinolates from Brassicaceae seeds and preparation of isothiocyanate and amine metabolites. *J Sci Food Agr*, **86**, 1271-80.

Sharifia A M, Eslami H, Larijani B, et al (2009). Involvement of caspase-8, -9, and -3 in high glucose-induced apoptosis in PC12 cells. *Neuroscience Lett*, **459**, 47-51.

Troncoso R, Espinoza C, Sánchez-Estrada A, et al (2005). Analysis of the isothiocyanates present in cabbage leaves extract and their potential application to control Alternaria rot in bell peppers. *Food Res Int*, **38**, 701-8.

Vaughn SF, Berhow MA (2005). Glucosinolate hydrolysis products from various plant sources: pH effects, isolation, and purification. *Ind Crops Prod*, **21**, 193-202.

Wang N, Qu T, Shen L, et al (2010). In-silico study of 4-methylsulfinyl-3-butenyl isothiocyanate binding to tubulin induces A549 cells apoptosis. *Acta Pharmaceutica Sinica*, **45**, 934-9.

Wang N, Shen LQ, Qiu SX, et al (2010). Analysis of the isothiocyanates present in three Chinese Brassica vegetable seeds and their potential anticancer bioactivities. *Eur Food Res Technol*, **231**, 951-8.

Xia D, Fangshi Z, Yun Yang, et al (2013). Purification, antitumor activity in vitro of steroidal glycoalkaloids from black nightshade (*Solanum nigrum* L.). *Food Chem*, **141**, 1181-6.

Xi Z, Shen L L, Zhou J Y, et al (2012). Beta-asarone induces lovo colon cancer cell apoptosis by up-regulation of caspases through a mitochondrial pathway in vitro and in vivo. *Asian Pacific J Cancer Prev*, **13**, 5291-8.

Zhu Y, Zhuang J X, Wang Q, et al (2013). Inhibitory effect of benzyl isothiocyanate on proliferation in vitro of human glioma cells. *Asian Pacific J Cancer Prev*, **14**, 2607-10.